

# Photodissociation of semiconductor positive cluster ions

Q.-L. Zhang,<sup>a)</sup> Y. Liu,<sup>a)</sup> R. F. Curl, F. K. Tittel, and R. E. Smalley

*Rice Quantum Institute, Departments of Chemistry and Electrical Engineering, Rice University, Houston, Texas 77251*

(Received 29 July 1987; accepted 16 October 1987)

Laser photofragmentation of Si, Ge, and GaAs positive cluster ions prepared by laser vaporization and supersonic beam expansion has been investigated using tandem time-of-flight mass spectrometry. Si clusters up to size 80, Ge clusters to size 40, and GaAs clusters up to a total of 31 atoms were studied.  $\text{Si}_n^+$  and  $\text{Ge}_n^+$  for  $n = 12$ –26 give daughter ions of about half their original size. For both Si and Ge, this apparent positive ion fissioning appears to go over with increasing  $n$  to neutral loss of seven and ten, but for  $\text{Si}_n^+$  the range of  $n$  values where this is observed is rather small. At low fluences, the larger  $\text{Ge}_n^+$  clusters up to the maximum size observed (50) sequentially lose  $\text{Ge}_{10}$  (and in some cases with lower intensity  $\text{Ge}_7$ ). Larger  $\text{Si}_n^+$  clusters ( $n > 30$ ) always fragment primarily to produce positive ion clusters in the 6–11 size range with a subsidiary channel of loss of a single Si atom. At high laser fluences,  $\text{Ge}_n^+$  also fragments to produce primarily positive ion clusters in the 6–11 size range with an intensity pattern essentially identical to  $\text{Si}_n^+$  at similar fluences.  $\text{Ga}_x\text{As}_y^+$  clusters lose one or more atoms in what is probably a sequential process with positive ion clusters in which the total number of atoms,  $x + y$ , is odd being more prominent.

## I. INTRODUCTION

A number of theoretical and experimental studies<sup>1–11</sup> aimed at understanding the structural properties of semiconductor neutral and ionic clusters have been carried out. There is a special interest in learning when and how the properties of the clusters approach those of the bulk materials as cluster size increases. This approach to the bulk can be expected to be different from metals and inert gas clusters,<sup>1</sup> because the semiconductor elements, Si and Ge, are covalent with  $sp^3$  hybridization directional bonds. When the clusters of these elements are produced, one may expect that they would have bonding resembling the network structure of the bulk. However, the unsatisfied valences at the surface should force reconstruction of surface layers. Since the cluster sizes we are talking about have less than 100 atoms, most of the atoms of a cluster are on the surface<sup>2</sup> and the reconstruction is likely to be so extensive that the structure of the cluster could bear little resemblance to the bulk. Several models for the mechanism of cluster formation and of cluster structures based on calculation<sup>1–4</sup> and experimental results<sup>5–10</sup> have been proposed.

The study of the photofragmentation of mass selected positive and negative cluster ions offers the prospect of learning something about the structure and bonding of the clusters. In previous work of this sort, Bloomfield, Freeman, and Brown have carried out photofragmentation studies<sup>8</sup> of hot  $\text{Si}_n^+$  clusters with  $n < 13$  produced by ionizing neutral clusters with ArF laser (6.4 eV) just before ion extraction. They found that fragmentation is primarily into  $\text{Si}_4^+$ ,  $\text{Si}_6^+$ , and  $\text{Si}_{10}^+$ . In this laboratory, we have studied laser detachment and photofragmentation of negative cluster ions of Si, Ge, and GaAs of size up to about 30 atoms.<sup>7</sup> Phillips<sup>11</sup> has interpreted this negative ion photofragmentation data as indicat-

ing the existence of trilayer of five-, six-, and seven-membered rings for clusters of size 15, 18, and 21, respectively.

If one wishes to learn about the transition to bulk properties, it seems clearly desirable to extend these studies to larger cluster sizes for either positive or negative ions. Thus in the present work, we report similar photofragmentation studies on cluster positive ions of Si, Ge, and GaAs as large as 80 atoms (for Si). These ions are produced directly by laser vaporization prior to supersonic expansion, and therefore should be substantially cooled by supersonic expansion and be in a well-defined internal state at the point of laser interrogation.

These studies also provide some interesting additional information about the validity of using photoionization detection of neutral semiconductor cluster beams. It is quite clear that extensive fragmentation can occur. The question of how such fragmentation might be minimized is discussed at the end of this paper.

## II. EXPERIMENTAL

The apparatus used in this experiment has been described elsewhere.<sup>12</sup> Briefly, material is pulse vaporized from a rotating semiconductor disk by the output of the second harmonic of a Nd:YAG laser (25 mJ/pulse, 5 ns pulse width). The vaporization takes place in the center of a pulse of helium carrier gas (backing pressure 8 atm) which entrains the hot plasma produced by the laser. The mixture flows into a clustering and thermalization region which is then followed by free expansion in a vacuum. The resulting supersonic jet is skimmed into a molecular beam containing both neutral clusters and positive and negative cluster ions. Positive cluster ions are extracted from the supersonic molecular beam into a 3 m long time-of-flight tube.  $\text{Si}_n^+$  ions of size up to 80 are readily produced by this method, but it is more difficult to obtain large clusters of Ge and GaAs, and

<sup>a)</sup> Robert A. Welch Foundation Predoctoral Fellow.

the largest usable cluster ion of Ge is  $\sim 50$  atoms and of GaAs is  $\sim 40$  atoms.

The mass spectrum of the positive cluster ions can be obtained by a in-line detector, or the clusters can be mass gated, decelerated, and probed by the second laser (UV or visible). The photodissociation products are accelerated into a perpendicular time-of-flight tube and collected at the end of the tube by two MCP-409 microchannel plates. The positive cluster ions were probed with the second (532 nm), third (355 nm), and fourth (266 nm) harmonics of a Q-switched Nd:YAG laser and with the KrF (249 nm) and ArF (193 nm) excimer laser lines. In these experiments the laser was never focused. For the excimer laser lines, the excess beam area was removed by a blocking mask. The beam areas for all fragmentation lasers was approximately  $1 \text{ cm}^2$ . The pulse length of the Nd:YAG harmonics is  $\sim 5 \text{ ns}$  and of the two excimer lines is about  $\sim 15 \text{ ns}$ .

### III. RESULTS

We have available a wide range of fragmentation laser wavelengths (Nd:YAG second, third, and fourth harmonics and excimer wavelengths KrF and ArF) and a wide range of fragmentation laser fluences. As a general observation for all three systems studied, the nature of the fragmentation patterns does not depend qualitatively upon the fragmentation laser used, although there are significant dependences upon fragmentation laser fluence which occur at different fluences for different lasers. In other respects, the different substances exhibit different behaviors (although there are remarkable similarities between Si and Ge). Below we will describe the observations for GaAs, Si, and Ge in turn.

#### A. Fragmentation of GaAs positive cluster ions

Figure 1 shows the mass spectrum of GaAs positive cluster ions produced by 532 nm laser vaporization. The feeble even/odd alternation reported<sup>7</sup> in the negative ions is not found for the positive ion distribution.

Figure 2 depicts the fragmentation pattern of  $\text{Ga}_x\text{As}_y$  with  $x + y = 31$  obtained by selecting this ion by time-of-flight using the mass gate. The fragmentation pattern shown in Fig. 2 is very similar to the fragmentation of negative clusters.<sup>7</sup> In both patterns, ion fragments are observed corresponding to the loss of from 1 to nearly 30 atoms. With the increasing laser fluence, small daughter ions become more

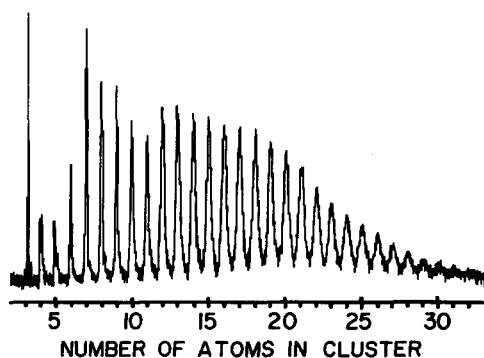


FIG. 1. Mass spectrum of GaAs positive ion clusters produced by 25 mJ/pulse 532 nm laser.

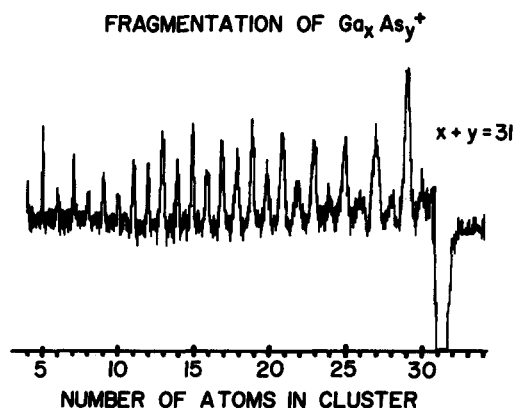


FIG. 2. Fragmentation of GaAs 31-atom positive ions with  $27 \text{ mJ/cm}^2$  third harmonic laser (355 nm). The pictures were obtained by subtracting two data sets: one with dissociation laser on and the other with laser off. Thus the parent ion peak shows a depletion. Even/odd alternation can be seen for all fragments.

prominent suggesting that perhaps daughter ions are dissociating further to give granddaughters. As depicted in Fig. 2, there is an even/odd alternation in the distribution of the fragments: Productions with an odd number of atoms are more intense than their neighboring products with an even number of atoms. This is also observed in the photofragmentation of GaAs negative cluster ions.

#### B. Fragmentation of Si positive cluster ions

The mass spectrum of Si positive cluster ions is presented in Fig. 3. Note that the intensity distribution for  $n > 20$  is uniform with no indication of any "magic numbers." When the photofragmentation is probed, an interesting change takes place as the parent cluster size reaches  $\text{Si}_{12}^+$ . For  $\text{Si}_{10}^+$  and  $\text{Si}_{11}^+$ , the largest ion fragments at low fluence are 6 and 7, respectively. When the fluence is increased moderately,  $\text{Si}_4^+$  and  $\text{Si}_5^+$  daughters have intensities comparable with  $\text{Si}_6^+$  and  $\text{Si}_7^+$  daughters. For clusters larger than 11 only 6–11 positive ion fragments are observed even at quite high fragmentation laser fluences. As shown in Fig. 4, in the range of 12 to 24, the  $\text{Si}_n^+$  often appear to photofragment by a fission process, e.g.,

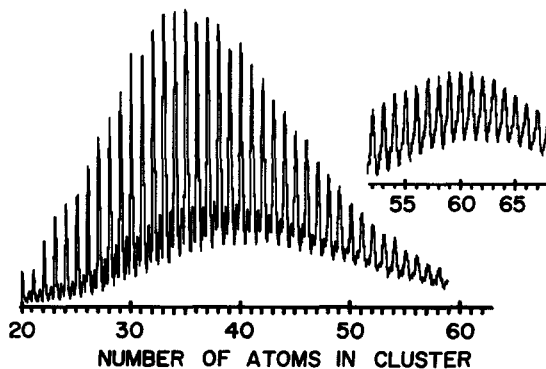


FIG. 3. Mass spectrum of Si positive ion clusters produced by 25 mJ/pulse second harmonic (532 nm) laser. The small peaks intermediate between the main cluster peaks are due to  $\text{Si}_n\text{O}^+$ .

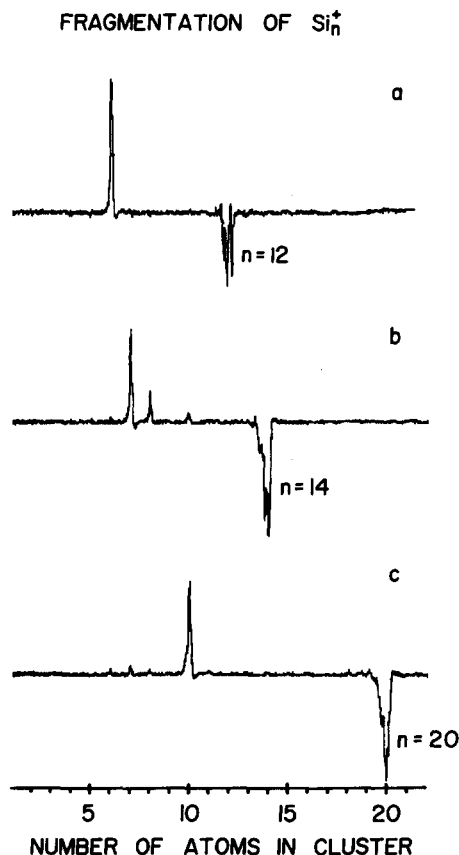


FIG. 4. Fragmentation of (a)  $\text{Si}_{12}^+$ , (b)  $\text{Si}_{14}^+$ , and (c)  $\text{Si}_{20}^+$  with  $23 \text{ mJ/cm}^2$  fourth harmonic (266 nm).



in a manner similar to  $\text{Si}_n^-$  fragmentation.<sup>7</sup> However, as will be illustrated for Ge which behaves in this respect very similarly, for some values of  $n$  there can be large differences between the positive and negative ion fissioning while for other cluster sizes the patterns are identical for the two charge states.

As  $n$  increases for  $\text{Si}_n^+$  above 23 atoms, more extensive fragmentation can be distinguished from the loss of ten atoms, and it is found for  $n = 23$ –29 that loss of ten atoms and loss of seven atoms are significant processes although fragmentation down of  $\text{Si}_n^+$  with  $n = 6$ –11 is always a significant process even at the lowest fluences. In this size region, loss of two or three Si atoms is also observable at the higher fluences.

Larger clusters ( $n > 30$ ) fragment both by apparent explosion down to  $\text{Si}_6^+ - \text{Si}_{11}^+$  and by the loss of one atom as seen in Fig. 5 for  $\text{Si}_{60}^+$ . Generally at low fluence,  $\text{Si}_{10}^+$  and  $\text{Si}_{11}^+$  are the most prominent small fragments as can be seen in the top trace of Fig. 5, while at higher fluence all 6–11 positive ions are present to about the same extent (bottom trace of Fig. 5). The  $\text{Si}_{60}^+$  fragmentation into  $\text{Si}_{10}^+$  by the ArF laser appears to be at least a two photon process as shown by the fluence dependence depicted in Fig. 6. We were unable to find conditions under which the larger  $\text{Si}_n^+$  clusters ( $n > 30$ ) showed intermediate fragments such as loss of  $\text{Si}_{10}$  as were found in the case of Ge (*vide infra*).

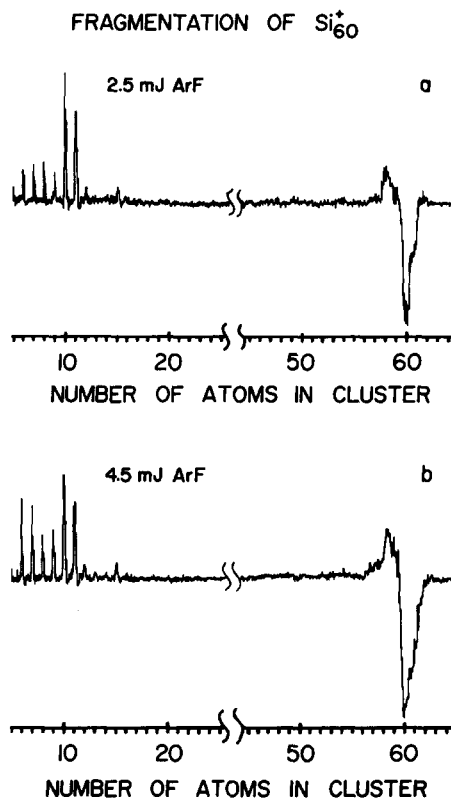


FIG. 5. Fragmentation of  $\text{Si}_{60}^+$  with (a)  $2.5 \text{ mJ/cm}^2$  ArF laser (193 nm); (b)  $4.5 \text{ mJ/cm}^2$  ArF laser. There are no discernable fragment peaks in the region not shown, and we are rather certain that we have observed all positive ion fragments. The relative intensities of fragments in the 6–11 region as compared with the parent depletion depends strongly on the deflection plate voltage. There is no single deflector voltage which produces relative intensities faithfully reproducing the relative ion fluxes over the entire mass region. Here the intensities at high masses are relatively too strong.

### C. Fragmentation of Ge positive cluster ions

The mass spectrum of Ge positive cluster ions is presented in Fig. 7. Again there is no indication of magic numbers in the positive ion distribution. The smaller  $\text{Ge}_n^+$  ions have virtually the same fissioning channels as  $\text{Si}_n^+$  and give rise in most cases to the same product ions. The larger  $\text{Ge}_n^+$  ions exhibit the same fragmentation channels as  $\text{Si}_n^+$ : loss of single atom and fragmentation into 6–11 positive ions with

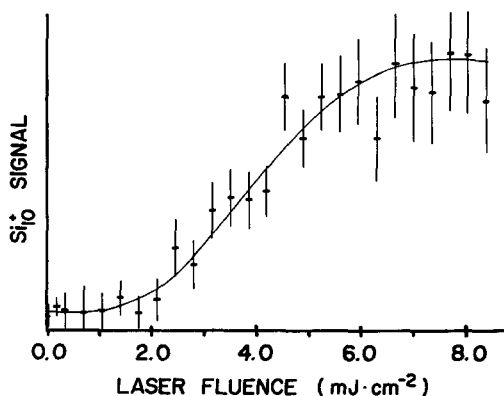


FIG. 6. Fluence dependence of  $\text{Si}_{10}^+$  signal intensities produced from  $\text{Si}_{60}^+$  with ArF (193 nm) laser.

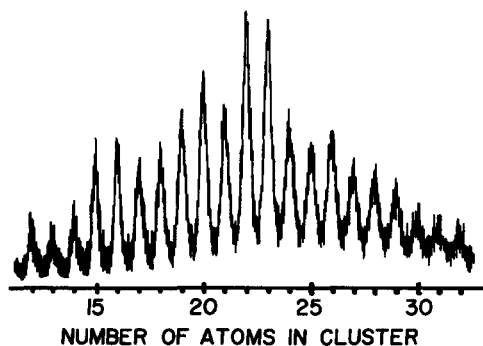


FIG. 7. Mass spectrum of Ge positive ion clusters produced by 25 mJ/pulse second harmonic of YAG laser (532 nm).

$\text{Ge}_{10}^+$  dominant in that size range. At very high fluences, only 6–11 positive ions are seen from the photofragmentation of any large positive ion for both Si and Ge, and the intensity patterns are remarkably similar as is illustrated in Fig. 8. Moreover, this fragmentation and intensity pattern is exactly as was previously found<sup>9</sup> for high fluence ArF photoionization of the neutral clusters as is repeated in Fig. 8. The photoion distributions in Figs. 8(c) and 8(d) are almost certainly dominated by fragmentation as evidenced by the tails to high mass on the 6–11 peaks which indicate that much of the signal arises from a higher mass ion which fragments during acceleration.

When photofragmentation of the larger ions at low fluence is explored, a richer and more interesting pattern is revealed than is the case for either Si or GaAs positive ions. The larger  $\text{Ge}_n^+$  species show a fragmentation corresponding to loss of  $\text{Ge}_{10}$  and to some extent  $\text{Ge}_7$ . Thus, as shown in

the upper panel of Fig. 9,  $\text{Ge}_{30}^+$  fragments at low fluence to produce almost exclusively  $\text{Ge}_{20}^+$  presumably by loss of neutral  $\text{Ge}_{10}$ . At higher fluence as shown in the lower panel of Fig. 9,  $\text{Ge}_{10}^+$  appears presumably by stepwise loss of  $\text{Ge}_{10}$  from  $\text{Ge}_{20}^+$  (in this context, it should be noted that mass-selected, cold  $\text{Ge}_{20}^+$  fragments to produce  $\text{Ge}_{10}^+$ ).  $\text{Ge}_{35}^+$  fragments primarily into  $\text{Ge}_{25}^+$  and  $\text{Ge}_{15}^+$ . On the other hand,  $\text{Ge}_{38}^+$  fragments almost equally into  $\text{Ge}_{31}^+$  and  $\text{Ge}_{28}^+$ . Figure 10 shows the fragmentation of  $\text{Ge}_{39}^+$  which appears to indicate loss of seven and ten neutrals, respectively ( $\text{Ge}_{32}^+$  and  $\text{Ge}_{29}^+$ ) in comparable amounts with these ions then losing a ten neutral ( $\text{Ge}_{22}^+$  and  $\text{Ge}_{19}^+$ ). Other clusters in this size region behave similarly generally favoring loss of  $\text{Ge}_{10}^+$ .

As we remarked above, qualitatively for clusters in the 12 to 25 size range, Ge positive and negative ions behave similarly to the corresponding Si positive and negative ions producing mostly the same daughters often in similar proportions. Moreover, the positive ions often exhibit the same fragmentation patterns as the corresponding negative ions. Thus  $\text{Ge}_{20}^+$ ,  $\text{Ge}_{20}^-$ ,  $\text{Si}_{20}^+$ , and  $\text{Si}_{20}^-$  all fragment to give only the ten ion of the same charge state. This similarity, however, is not uniform as illustrated in Fig. 11 where the fragmentation of  $\text{Ge}_{18}^+$  is compared with the fragmentation of  $\text{Ge}_{18}^-$ . Even though a higher energy per photon and fluence is used in fragmenting  $\text{Ge}_{18}^+$  than  $\text{Ge}_{18}^-$ , it can be seen that  $\text{Ge}_{18}^+$  produces primarily  $\text{Ge}_{11}^+$  while  $\text{Ge}_{18}^-$  produces  $\text{Ge}_{12}^-$ ,  $\text{Ge}_9^-$ , and  $\text{Ge}_6^-$  in roughly equal quantities with a lesser amount of  $\text{Ge}_{11}^-$  and several other negative ions. A comparison of the positive and negative ion fragmentation patterns is given in Table I. With the  $\text{Ge}_n^+$ , it is possible to observe fragmentation patterns up to  $n = 50$ ; the patterns observed in the range  $n = 31$ –50 are listed separately in Table II.

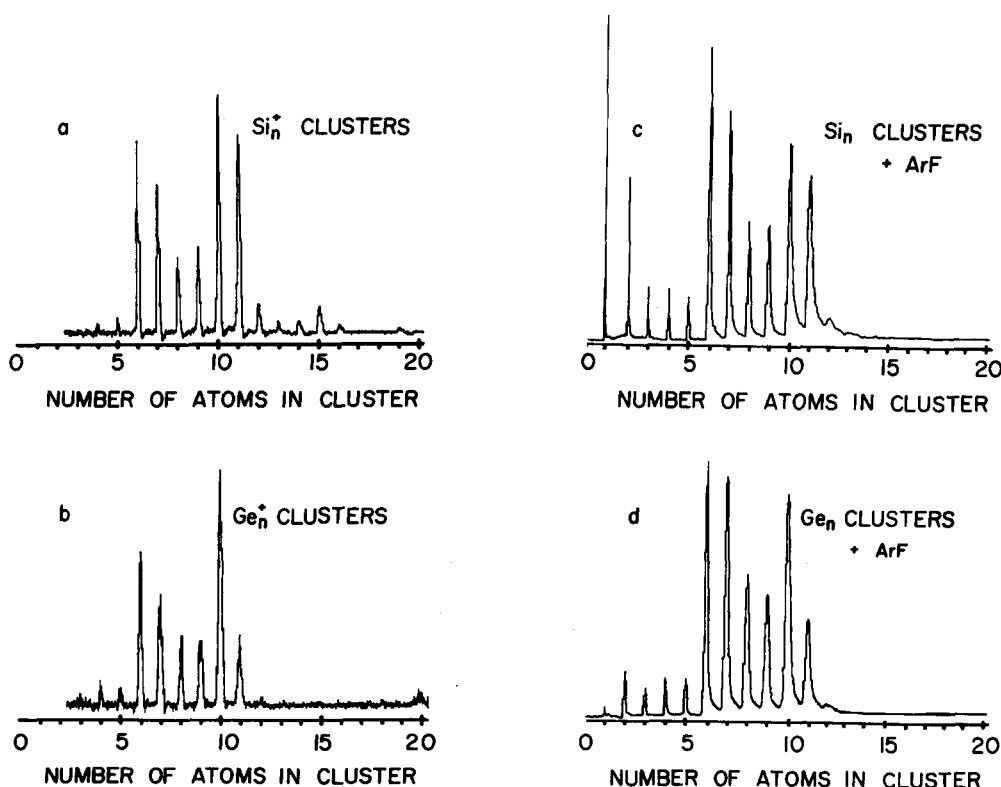


FIG. 8. (a) Fragmentation products in 6 to 11 size range coming from  $\text{Si}_{60}^+$  with 43 mJ/cm<sup>2</sup> third harmonic (355 nm) laser; (b) fragmentation products in 6 to 11 size range coming from  $\text{Ge}_{30}^+$  with 10 mJ/cm<sup>2</sup> KrF (248 nm) laser; (c) silicon neutral clusters ionized with 0.5 mJ/cm<sup>2</sup> ArF (193 nm) laser; (d) germanium neutral clusters ionized with 0.5 mJ/cm<sup>2</sup> ArF laser.

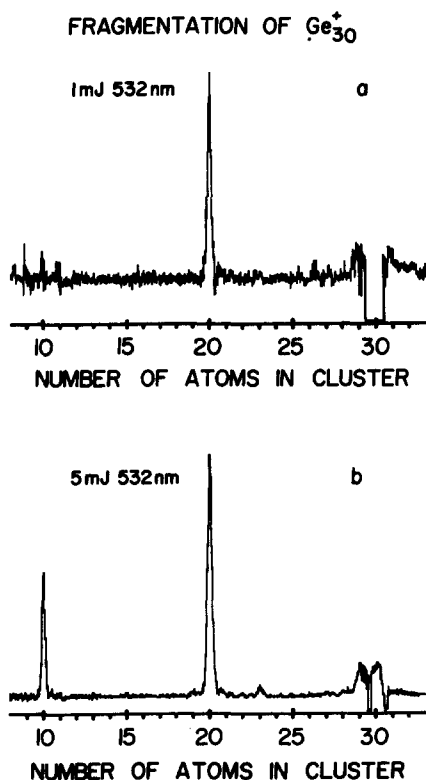


FIG. 9. Fragmentation of  $\text{Ge}_{30}^+$  with (a)  $1 \text{ mJ/cm}^2$  second harmonic of YAG (532 nm) laser; (b)  $5 \text{ mJ/cm}^2$  second harmonic of YAG laser.

#### IV. DISCUSSION

When one or more visible or UV photons are absorbed by a large semiconductor cluster ion, internal conversion of the electronic energy to vibrational energy should occur rapidly. Time resolved, two-color studies in which Si and Ge neutral clusters of unknown size (but probably in the range 12 to 30 atoms) were photoionized (and photofragmented) to  $\text{Si}_{10}^+$  and  $\text{Ge}_{10}^+$  showed a transient decaying in  $\sim 100 \text{ ns}$ .<sup>9</sup> In the present longer time scale ( $\sim 4 \mu\text{s}$ ) fragmentation experiments, if the energy absorbed exceeds the binding energy, then the ion should undergo internal conversion and fragment by an essentially statistical unimolecular decomposition process. Let us suppose that a  $\text{Si}_n^+$  cluster fragments into two pieces:

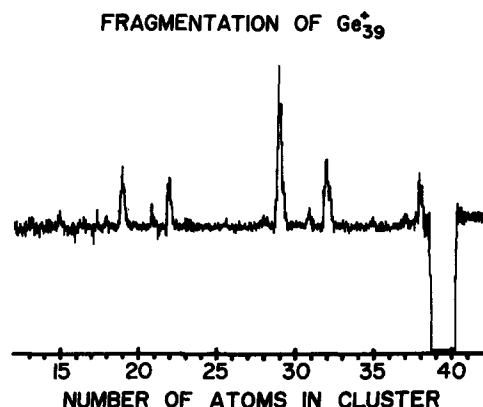


FIG. 10. Fragmentation of  $\text{Ge}_{39}^+$  with  $2 \text{ mJ/cm}^2$  third harmonic of YAG (355 nm) laser.

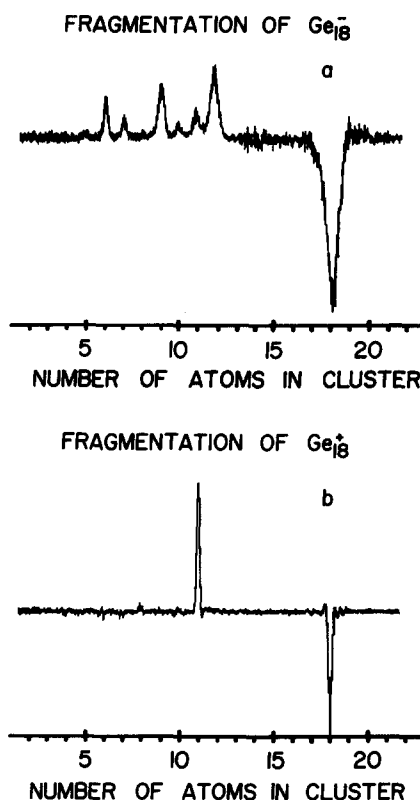
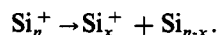


FIG. 11. Fragmentation of (a)  $\text{Ge}_{18}^-$  with  $3.5 \text{ mJ/cm}^2$  426 nm dye laser; (b)  $\text{Ge}_{18}^+$  with  $4 \text{ mJ/cm}^2$  third harmonic of YAG (355 nm) laser. The difference in linewidths between (a) and (b) is almost certainly caused by the experimental differences. The second drift tube in the tandem TOF for the negative ions was in-line instead of perpendicular. The acceleration voltages were also different.



The charge should go with the fragment for which the neutral has the lowest ionization energy because as the particles separate the electrons can tunnel from one to the other, and when the electron energy is lower, a larger volume of phase space is available because of the resulting excess nuclear motional energy. It is known that the ionization energy decreases with increasing cluster size, therefore the charge should appear on the larger fragment. Of course, it is always possible that a neutral fragment is ionized by the fragmentation laser, but such a mechanism, if present, would not account for the absence of large positive ion fragments.

When  $\text{Si}_{60}^+$  is fragmented and, aside from a small amount of  $\text{Si}_{59}^+$ , all the charged species are in the 6–11 size range, the almost inescapable conclusion appears to be that  $\text{Si}_{60}^+$  has fragmented into many small pieces none larger than 11 atoms. One possible explanation of this would seem to be that  $\text{Si}_{60}^+$  is a loosely bound aggregate of smaller clusters in the 6–11 size range. However, photofragmentation of  $\text{Si}_{60}^+$  on a  $4 \mu\text{s}$  times scale is a *two-photon process with 6.4 eV photons*—an observation which does not seem consistent with such a loosely bound aggregate.

A very difficult question to answer is whether the fragmentation to the 6–11 size range takes place in a single step as a sort of explosion or if it involves a sequence of intermedi-

TABLE I. Fragmentation channels<sup>a</sup> of  $\text{Si}_n^+$ ,  $\text{Si}_n^-$ ,  $\text{Ge}_n^+$ ,  $\text{Ge}_n^-$ .

<i>n</i>	Products $\text{Si}_x^+$ of $\text{Si}_n^+$ 266 nm	Products $\text{Si}_x^-$ of $\text{Si}_n^-$ 355 nm	Products $\text{Ge}_x^+$ of $\text{Ge}_n^+$ 266 nm	Products $\text{Ge}_x^-$ of $\text{Ge}_n^-$ 355 nm
10	<b>6</b> , <sup>b</sup> 4, 7, 5 <sup>c</sup>	none	<b>6, 7, 4, 8, 9, 5</b>	4, 6, 5
11	7, <b>6</b> , 5, 4, 10	<b>5, 4, 6</b>	7, <b>6</b> , 5, 10, 4	5, 4, 6
12	<b>6</b>	<b>6, 5</b>	<b>6, 7</b> , trace 8, 10, 11	6, 5
13	7, <b>6</b> , 12	<b>6, 7</b>	6, 7, 3, weaker 11, 12	6, 7
14	7, 8, 10, 6	7, 10, 8	7, 8, 6, 9	7, 10
15	8, 9	9, 5	8, 9, 10	9, 5
16	<b>10, 6, 4</b>	10	<b>10, 6</b>	10
17	<b>10, 11, 7</b>	10	<b>10, 7, 6, 11</b>	10
18	<b>11, 15, 17, 8</b>	12, 6, 7, 9, 11	<b>11</b> , trace 6–10	12, 9, 6, 11, 7, 10, 5
19	9, 10, 6, 7, 12, 13, 16	9, 10, 6	9, 10, 11, 12, 18, 7	9, 6, 10
20	<b>10</b> , trace 6–11	10	<b>10</b> , trace 6–11	10
21	<b>11</b> , trace 6–10	5, 9, 10, 11, 14, 15	11, trace 6–10	11, 5, 7, 10
22	12, 15, 10, 6, weaker 11, 8, 9, 16	10, 16, 6, 9, 5	6, 8, 12, 15, 10 11, 7, 9, 5, 4	16, 9, 10
23	10, 13, 11, 16, 6, 7		6, 7, 10, 13, 16 trace 8, 9, 11, 12	
24	<b>14, 11, 7, 10</b>		<b>14, 7, 10, 6, 8, 11</b>	
25	<b>15</b> , trace 23, 6–11		<b>15, 8</b> , weaker 6–11	
26	<b>10, 16, 19, 6–11</b>		<b>10, 16, 6–11, 15</b>	
27	<b>10, 11, 15, 14, 17, 24, 25</b>		<b>10, 20, 6–11, 15, 17, 16</b>	
28	<b>11, 10, 12, 8, 6, 18, 22, 26</b>		<b>11, 6–10, 18, 21, 26, 15, 16</b>	
29	10, 11, 9, 7, 6, 8 16, 19, 27, 23		9, 6–11, 19, 22, 12, 15, 16	
30	10, 11, 6–9, 14, 15, 16, 20		<b>20, 10</b> , trace 6–11	

<sup>a</sup> The products and their relative intensities of a positive cluster will change with laser fluence, usually we list the results obtained for the laser fluence as low as practical.

<sup>b</sup> Boldface type indicates that this daughter is of much higher intensity than the others.

<sup>c</sup> The products are listed in the order of decreasing intensity.

ate steps involving the loss of seven or ten atoms, which are evident in Si up to about 30 atoms and in Ge up to the largest size observable ( $n = 50$ ). We suspect that the fragmentation to the size range 6–11 and the sequential loss of ten (and seven) neutrals are two different processes because we always see the same essentially identical characteristic fragmentation pattern of 6–11 atom ions at high laser fluence for both Si and Ge clusters even though we can, for example as shown in Fig. 12, obtain almost dominant  $\text{Ge}_{10}^+$  from the fragmentation of  $\text{Ge}_{30}^+$  at lower fluences (we also have

TABLE II. Fragmentation channels of  $\text{Ge}_n^+$  ( $30 < n < 51$ ).

<i>n</i>	Products $\text{Ge}_x^+$ of $\text{Ge}_n^+$	Laser and fluence
31	11, 21, 30 <sup>a</sup>	1 mJ 532 nm
32	<b>22</b> , <sup>b</sup> trace of 31, 21, 15	1 mJ 532 nm
33	23, 22, 32, 31	4 mJ 532 nm
34	<b>24, 14</b> , 23, 33, 27, 16, 15, 20	0.5 mJ 355 nm
35	<b>25, 15</b> , 28, 34, 24, 20, 14	0.5 mJ 355 nm
36	<b>26, 15</b> , 16, 35	0.5 mJ 355 nm
37	<b>10, 27, 20, 26</b> , 16, 17, 22, 36, 32, 30	2 mJ 355 nm
38	<b>11, 28, 31</b> , 37, 21, 20, 18, 23, 27	2 mJ 355 nm
39	29, 19, 32, 22, 38, 31, 21	2 mJ 355 nm
40	<b>10, 20, 30</b> , 11, 38, 19, 28, 29, 37	12.5 mJ 532 nm
45	15, 25, 35	2 mJ 355 nm
50	6, 10, 7, 8, 11, 9, 20	20 mJ 355 nm

<sup>a</sup> The products are listed in the order of decreasing intensity.

<sup>b</sup> Boldface type indicates that this daughter is of much higher intensity than the others.

$\text{Ge}_{10}^+ - \text{Ge}_{11}^+$  visible weakly when  $\text{Ge}_{10}^+$  is dominant). This suggests to us that the high fluence fragmentation may be an explosion into many small pieces, rather than a sequential loss of smaller neutrals.

The fact that loss does not stop at an intermediate stage for  $\text{Si}_n^+$  seems to imply that the activation energy necessary for the loss of the small fragment is high but is largely recovered as vibrational excitation of the larger piece as the fragments separate so that the excess energy remains high and unimolecular decay can continue. If the activation barrier is an “entrance channel” one, one would expect such behavior because for entrance channel barriers the exoergicity from the top of the barrier to products tend to be redistributed randomly in the products. For a small cluster product and a large cluster product, most of this energy should go into vibrational excitation of the large fragment. Presumably the high activation energy is required to break the half-dozen or more covalent bonds connecting the smaller fragment to tie up the resulting dangling bonds. Since it seems to be impossible to catch the fragmentation of  $\text{Si}_n^+$  at an intermediate stage, there is a strong suggestion that the activation energy for loss of a fragment like  $\text{Si}_{10}$  decreases as the cluster size decreases.

The observations on the fragmentation of  $\text{Ge}_n^+$  suggest another channel corresponding to a sequence of losses of  $\text{Ge}_{10}$  until  $\text{Ge}_m^+$  fissions into two pieces in the 6–11 range. At this point apparently either the activation energy increases

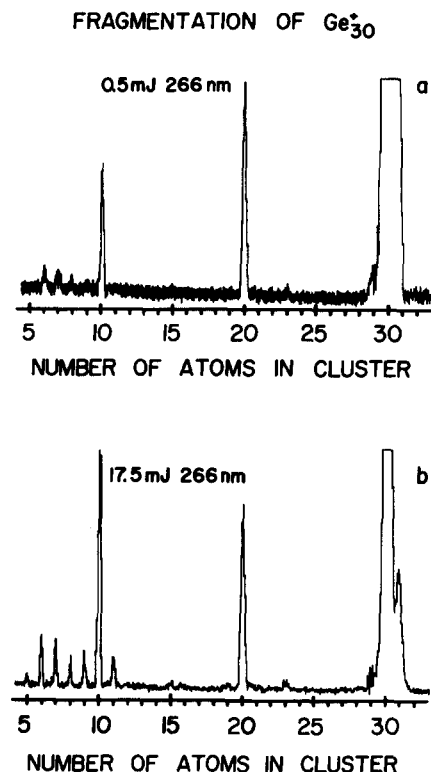


FIG. 12. Fragmentation of  $\text{Ge}_{30}^+$  at (a) 0.5 mJ/cm<sup>2</sup> and (b) 17.5 mJ/cm<sup>2</sup> of the fourth harmonic of YAG (266) laser showing the apparent superposition of a low fluence sequential loss of  $\text{Ge}_{10}$  and a high fluence fragmentation into  $\text{Ge}_6^+ - \text{Ge}_{11}^+$ . This figure is not a fragmentation laser-on minus laser-off depiction, but instead consists of all laser-on shots.

or surface restructuring is less effective or when the energy is equally divided between two equal size particles insufficient energy remains for fragmentation of the charged particle on the experimental time scale. At any rate fragmentation ceases as very few charged clusters smaller than six atoms are observed upon fragmentation of large Si and Ge clusters at any fluence employed even though such species are observed when 6–11 clusters are singled out and photofragmented.

How do sequential losses of  $\text{Ge}_{10}$  come about? Is it because  $\text{Ge}_{10}$  is exceptionally stable or are there in some way  $\text{Ge}_{10}$  subunits in the clusters with natural cleavage planes allowing such subunits to fall out? There is insufficient information to answer this question, but our intuition suggests that both causes are probably at work. The fragmentation patterns for  $\text{Ge}_n^+$  and  $\text{Ge}_n^-$  with  $n = 18$ –24 suggest that  $\text{Ge}_{10}$  may be more stable than most of the clusters of neighboring sizes but not exceptionally so. On the other hand, the stresses caused by surface restructuring may produce internal strains leading to natural cleavage planes in the cluster. As a ten atom adamantane cage structure is a natural subunit of the diamond lattice, it would not be surprising if cleavage started in a direction which might cleave off such a subunit. With an entrance channel barrier, as cleavage starts and restructuring begins (i.e., the top of the activation barrier is passed), the large energy being released could be randomized permitting the system to search for the lowest ener-

gy channel accessible from that point thereby bringing a special stability of  $\text{Ge}_{10}$  into play.

Referring to Table I, we have already marked, that for cluster sizes where they can be compared, the fragmentation patterns of positive and negative ions are usually similar with some notable exceptions. Very recently Phillips<sup>11</sup> discussed structural models for Si and Ge clusters. In particular, examining the negative ion fragmentation data,<sup>7</sup> he note that the fragmentation of clusters of size 15, 18, and 21 seemed to follow a different pattern than the other clusters in the size range from 14 to 22. Phillips interpreted these differences as suggesting a trilayer ring structure of five-, six-, and seven-membered rings for 15, 18, and 21 respectively. Examining Table I, we see that there is an almost consistent pattern in which the dominant charged fragments for  $n = 14, 16, 17, 19$ , and 20 are the same for both positive and negative ions while there is a large dependence of fragmentation pattern upon charge state for  $n = 15, 18, 21$ , and 22. It is probably too early to tell whether this is significant. An alternate empirical correlation is that in this region the dominant fragments usually correspond in the case of the fragmentation of positive ions to either the loss of  $\text{X}_7$  or  $\text{X}_{10}$  ( $n = 16$  which gives  $\text{X}_{10}^+$  is the only exception) and in the case of negative ions to either the loss of  $\text{X}_6$  or  $\text{X}_{10}$  ( $n = 14$  which gives  $\text{X}_7^-$  and  $n = 17$  which gives  $\text{X}_{10}^-$  are the exceptions).

Very different from Si and Ge is GaAs positive and negative cluster ion photofragmentation. The sequential loss of single atoms seems to be involved much as is observed in metal positive cluster ion photofragmentation.<sup>13</sup> Since GaAs also forms a covalent solid with the diamond structure, this resemblance to metals rather than Si and Ge at first seems somewhat surprising. However, it may be explainable by the fact that GaAs can restructure by introducing ionic bonding and changing the hybridization at Ga and As.

The odd-even intensity alternation with the odd more intense observed here with the positive GaAs ion fragmentation and observed<sup>7</sup> previously with negative GaAs ion can again be interpreted as suggesting<sup>7</sup> that all the dangling bonds are tied up for the cluster ions containing an even number of electrons (those with an odd number of atoms). Recent photoelectron studies<sup>14</sup> of  $\text{Si}_n^-$  and  $\text{Ge}_n^-$  suggest that many even  $n$  neutral  $\text{Si}_n$  and  $\text{Ge}_n$  clusters have open shell electronic structures. The odd-even intensity alternation found here suggests that this may not be the case for GaAs. Perhaps, this again suggests that GaAs is different from Si and Ge because surface reconstruction may be carried out to a greater extent by changes in formal charge with corresponding changes in hybridization for GaAs.

Photoionization is widely used to detect neutral cluster beams. It is very important that the detection scheme faithfully reproduce the neutral cluster distribution. It is already known<sup>9</sup> that photofragmentation is extensive with ArF laser photoionization detection of Si and Ge cluster beams very strongly biasing the apparent distribution to clusters in the 6 to 11 size range and the work reported here provides verification of this. The previous work on negative ion photodetachment and photofragmentation<sup>7</sup> indicates that ionization (or for the negative ions, detachment) becomes much more important than fragmentation as the probe laser photon energy

becomes significantly larger than the ionization threshold, and the previous study<sup>9</sup> of Si and Ge cluster beams which shows much smoother distributions of cluster ions for F<sub>2</sub> laser (157 nm) than for ArF laser (193 nm) is consonant with this. Trevor *et al.*<sup>10</sup> have discussed the conditions needed for photoionization detection to reflect faithfully the neutral distribution in somewhat more detail. It seems very clear that it is important to use an ionizing wavelength well above (perhaps 2 eV) the ionization threshold at as low a fluence as is feasible.

## ACKNOWLEDGMENTS

This work was supported by the U. S. Army Research Office, and the Robert A. Welch Foundation. The apparatus was constructed with the support of the National Science Foundation and the Department of Energy.

- <sup>1</sup>J. C. Phillips, *Chem. Rev.* **86**, 619 (1986).
- <sup>2</sup>C. M. Weinert, *Surf. Sci.* **156**, 641 (1985).
- <sup>3</sup>J. C. Phillips, *J. Chem. Phys.* **83**, 3330 (1985).
- <sup>4</sup>K. Raghavachari, *J. Chem. Phys.* **84**, 5672 (1986).
- <sup>5</sup>T. P. Martin and H. Schaber, *J. Chem. Phys.* **83**, 855 (1985).
- <sup>6</sup>S. C. O'Brien, Y. Liu, Q. Zhang, J. R. Heath, F. K. Tittel, R. F. Curl, and R. E. Smalley, *J. Chem. Phys.* **84**, 4074 (1986).
- <sup>7</sup>Y. Liu, Q. Zhang, F. K. Tittel, R. F. Curl, and R. E. Smalley, *J. Chem. Phys.* **85**, 7434 (1986).
- <sup>8</sup>L. A. Bloomfield, R. R. Freeman, and W. L. Brown, *Phys. Rev. Lett.* **54**, 2246 (1985).
- <sup>9</sup>J. R. Heath, Y. Liu, S. C. O'Brien, Q. Zhang, R. F. Curl, F. K. Tittel, and R. E. Smalley, *J. Chem. Phys.* **83**, 5520 (1985).
- <sup>10</sup>D. J. Trevor, D. M. Cox, K. C. Reichmann, R. O. Brickman, and A. Kaldor, *J. Phys. Chem.* **91**, 2598 (1987).
- <sup>11</sup>J. C. Phillips, *J. Chem. Phys.* **87**, 1712 (1987).
- <sup>12</sup>S. C. O'Brien, J. R. Heath, R. F. Curl, and R. E. Smalley, *J. Chem. Phys.* (submitted).
- <sup>13</sup>P. J. Brucat, L.-S. Zheng, C. L. Pettiette, S. Yang, and R. E. Smalley, *J. Chem. Phys.* **84**, 3078 (1986).
- <sup>14</sup>O. Cheshnovsky, S. H. Yang, C. L. Pettiette, M. J. Craycraft, Y. Liu, and R. E. Smalley, *Chem. Phys. Lett.* (in press).